

Electronic structure and electron-paramagnetic-resonance properties of intrinsic defects in GaAs

C. Delerue

*Laboratoire de Physique des Solides, Institut Supérieur d'Electronique du Nord, 41 boulevard Vauban,
59046 Lille CEDEX, France*

(Received 8 July 1991)

The electronic structure of vacancies, antisites, self-interstitials, and some related complex defects in GaAs is calculated using a self-consistent semiempirical tight-binding technique. In particular, we give the electron densities on the various atoms to predict the electron-paramagnetic-resonance properties of the defect. The interpretations of existing experimental spectra are reexamined.

I. INTRODUCTION

In III-V semiconductors the expected intrinsic point defects are vacancies, self-interstitials, and antisite defects. Complexes based on these elemental point defects are also likely to occur. In spite of many important studies, the microscopic identification of the intrinsic defects in GaAs is still far from complete. In effect, the electron paramagnetic resonance (EPR) technique, which is largely used to identify point defects in silicon for example, cannot be applied easily in GaAs. The obtained spectra are very broad and difficult to interpret. Consequently, there is no direct evidence at the present time that a single isolated point defect such as a vacancy, self-interstitial, or an antisite defect has been observed. For instance, the midgap electron trap EL2 found in most GaAs materials is still a matter of continuing debate.

Theoretically, several works using local-density methods¹⁻⁴ have been applied to the study of intrinsic point defects in GaAs. They particularly give information about energy levels and defect formation energies. In some cases, the atomic structure corresponding to the energy minimum is discussed.^{3,4} Nevertheless, this information is not always sufficient to help for a clear identification of defects from the experimental data. In particular, the calculated *s* and *p* electronic densities on the central and ligand atoms are not always available although they could be compared with the experimental densities obtained from the analysis of the hyperfine tensors. In addition, the local density techniques do not give the energy levels with a sufficient accuracy for the experimentalists. One reason for this is the well-known band-gap problem.⁵ Therefore results obtained with other techniques are necessary to provide additional information and to give an estimate of the discrepancy between the theories. Among these techniques, self-consistent semiempirical tight-binding calculations have been used with success to describe some point defects in semiconductors.^{6,7}

The purpose of this paper is to report a systematic theoretical calculation of the electronic structure of several intrinsic point defects in GaAs. The various charge states are examined within a self-consistent tight-binding Green's function technique. The energy levels,

their symmetry, and their localization on the central and neighbor atoms will be given with the aim to supply some useful information to the experimentalists. The analysis of the existing experimental data will be done in the light of these results. We show that the identification of many defects is uncertain.

II. THE CALCULATIONAL METHOD

Our calculation is based on the Green's function technique in the tight-binding approximation. This method has already been used, for instance, for the isolated dangling bond in silicon,⁸ transition-metal impurities,⁶ and the phosphorus vacancy in InP.⁹ The perfect GaAs crystal is described in an *s,p* atomic basis. The corresponding Hamiltonian is calculated with the parameters of Talwar and Ting,¹⁰ and the Green's functions G_0 are obtained by numerical integration over the Brillouin zone. Then the defect is created by application of the *ad hoc* perturbation potentials. For this, we use the Dyson equation

$$G = G_0 + G_0 V G, \quad (1)$$

where G is the perturbed Green's function and V the perturbation or the coupling matrix. In any case, the defect potential—or energy—is written as a sum of two contributions

$$V = V_b + V_s, \quad (2)$$

where V_b is the bare perturbation and V_s is the self-consistent potential which is adjusted after an iterative procedure. The form of the bare perturbation matrix depends on the defect. In the case of the vacancies and the antisites we consider in the matrix of V_b only diagonal elements. The vacancy is obtained by applying an infinite potential on the removed atom.¹¹ For an X_Y antisite defect ($X_Y = \text{As}_{\text{Ga}}$ or Ga_{As}), the replacement of a Y atom by an X atom is simulated by intraatomic potentials ΔE_s and ΔE_p on the *s* and *p* orbitals of the corresponding atom Y . ΔE_s and ΔE_p are taken as the differences between the X - and Y -atom energies in the crystal which are given by the parameters of Talwar and Ting.¹⁰ In the case of an X interstitial ($X = \text{As}$ or Ga), V_b is the coupling matrix of the interstitial atom with its neighbors. The interstitial atom

is represented by one s and three p orbitals whose energies are derived once again from the parameters of the bulk crystal.¹⁰ The couplings with the first neighbors ($d_1 = 2.43 \text{ \AA}$) and the second neighbors ($d_2 = 2.81 \text{ \AA}$) are considered. The interaction parameters $V(d_1)$ with the first neighbors are deduced from the Harrison's rules.¹² For the parameters $V(d_2)$ with the second neighbors, we use a classical scaling law:

$$V(d_2) = V(d_1) \exp \left[-2.5 \left(\frac{d_2}{d_1} - 1 \right) \right]. \quad (3)$$

The use of an exponential dependence and a value of 2.5 for the decay parameter is discussed in Ref. 13. For the self-consistent potential V_s , we have only considered diagonal terms as it is usually done in semiempirical tight-binding techniques.¹⁴ A self-consistent potential V_s^i is applied on all the defect atoms and their first neighbors i (for the interstitial), the self-consistency is extended to the second neighbors). V_s^i is linearly dependent on the net electronic population n_i on the atom i :

$$V_s^i = U(n_i - n_i^0), \quad (4)$$

where U is the average Coulomb energy and n_i^0 is the electronic population of the same atom in the bulk crystal. We have calculated $n_i^0 = 3.22$ for a gallium atom and $n_i^0 = 4.78$ for an arsenic atom. We have taken $U = 10 \text{ eV}$. We have checked that the accuracy of the results is insensitive to the exact value of this parameter.⁶ Usually, another way to do a self-consistent calculation is to impose the local neutrality on each atom.^{6,9} We have also verified that, in the case of the single vacancies, the two approaches of the self-consistency give very close results. But in the case of complex defects, the notion of local neutrality is less obvious: it explains why we did not use this method. For each defect we have calculated the ionization levels using the Slater's transition state,¹⁵ i.e., for a half-integer occupancy number.

III. ARSENIC VACANCY IN GaAs

In this section we present our results for the charged and neutral arsenic vacancy V_{As} in GaAs. The calculations are done for the undistorted and unrelaxed vacancy. Quite generally the level structure of the vacancies is now well known. It is mainly characterized by two states with a_1 and t_2 symmetry which can be in the forbidden band gap. These states are mainly formed by combinations of dangling bonds on the four neighbor atoms. The t_2 state has a threefold spatial degenerescence, the a_1 state is not degenerate. For the neutral As vacancy we get both the a_1 and t_2 levels in the band gap (a_1 at $E_v + 0.08 \text{ eV}$ and t_2 at $E_c + 0.96 \text{ eV}$). In that case, the a_1 and t_2 states, which are, respectively, populated by two and one electrons, are localized on the four Ga neighbors by 58 and 47%. We obtain five possible charge states V_{As}^+ , V_{As}^0 , V_{As}^- , V_{As}^{2-} , V_{As}^{3-} which correspond to 0,1,2,3,4 electrons on the t_2 state. The calculated ionization levels $\epsilon(3-/2-)$, $\epsilon(2-/1-)$, $\epsilon(1-/0)$, and $\epsilon(0/1+)$ are, respectively, at 1.26, 1.15, 1.04, and 0.83 eV with respect to the top of the valence band (see Fig. 1). We can compare

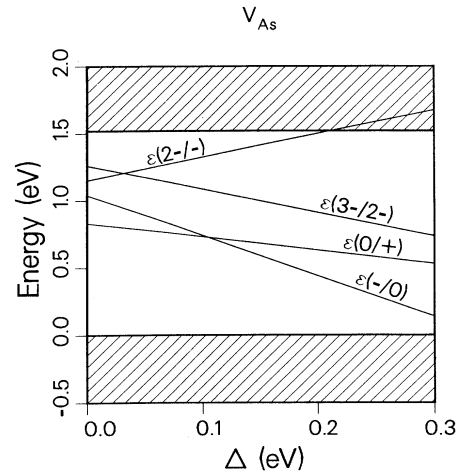


FIG. 1. Ionization levels for the distorted arsenic vacancy in GaAs. The levels are represented as function of the Jahn-Teller energy Δ . The top of the valence band is taken as reference for the energies.

these results with the existing literature. Our t_2 level energy for V_{As}^0 (0.96 eV) is in very good agreement with the energy obtained by the local density calculation of Bachelet, Baraff, and Schlüter¹ (1.08 eV) but our a_1 - t_2 splitting is lower (0.88 instead of 1.88 eV). It is well known that tight-binding methods underestimate this splitting compared to local density. In opposition to these results, Baraff and Schlüter² calculated the t_2 level in resonance in the conduction band and the a_1 level in the band gap. Therefore, they find only one ionization level $\epsilon(1+/2+)$ close to the valence band. Thus the spread of the results is important. Using another self-consistent tight-binding calculation, Xu and Lindefelt⁷ obtained results very close to ours, although their t_2 level is slightly higher. The occurrence of a t_2 level in the highest half part of the band gap is also confirmed by other calculations.^{16,17}

If, as predicted by our calculation, the various charge states of V_{As} correspond to changes in the occupancy of the t_2 level lying in the band gap, the Jahn-Teller distortions must be investigated. The determination of the stable atomic configurations would require, for instance, a calculation of the total energy: this is complex and cannot be done easily with tight-binding methods. However, a qualitative description of the distortions is possible in our view to characterize what could be the experimental properties of the defect. In particular, there is a competition between the electron-electron repulsion and the gain in energy resulting from the electron-lattice interaction which can lead in some cases to negative- U situations. This is particularly true for the vacancies, the silicon vacancy being a good example.¹⁸ For that purpose we use a simple model proposed by Lannoo¹⁹ to explain the role of the lattice distortions on defects with triply degenerate gap states. The triply degenerate state, here the t_2 state, can be populated by N_e electrons ($N_e = 0$ to 6). When it

is populated by one electron, a Jahn-Teller distortion splits the state into a lower nondegenerate component and an upper twofold degenerate one. The electron is in the lower state. With $N_e=2$, one adds the second electron in the same lower state. With $N_e=3$, the third electron must go into the upper twofold degenerate state, and a Jahn-Teller coupling to another lattice mode is expected. The same procedure is used for $N_e=4,5,6$. The total energy is expressed for each occupancy number as a function of a lattice coordinate Q and is minimized with respect to it. The one-electron level splittings corresponding to the energy minima are represented in Fig. 2 versus the electron filling N_e .

This model is simplified but is quite general. Details can be found in Ref. 19. The nature of the distortion—tetragonal or trigonal here—is not to be known. The occupancy levels $\epsilon(N_e+1, N_e)$ of the distorted system can be written as functions of the occupancy levels $\epsilon_0(N_e+1, N_e)$ in the absence of distortion and of the Jahn-Teller energy Δ [see Eq. (7) of Ref. 19]. One easily gets

$$\begin{aligned}\epsilon(1,0) &= \epsilon_0(1,0) - \Delta, \\ \epsilon(1,2) &= \epsilon_0(1,2) - 3\Delta, \\ \epsilon(3,2) &= \epsilon_0(3,2) + \frac{7}{4}\Delta, \\ \epsilon(4,3) &= \epsilon_0(4,3) - \frac{7}{4}\Delta, \\ \epsilon(5,4) &= \epsilon_0(5,4) + 3\Delta, \\ \epsilon(6,5) &= \epsilon_0(6,5) + \Delta.\end{aligned}\quad (5)$$

These levels for V_{As} are plotted versus Δ in Fig. 1 which shows an interesting behavior. For $\Delta < 0.03$ eV, the $\epsilon(3-/2-)$ level is lower than $\epsilon(2-/1-)$ and for $\Delta > 0.11$ eV, $\epsilon(0/1+)$ is lower than $\epsilon(1-/0)$. This means that we obtain a negative- U behavior for these charge states. Therefore, for $\Delta > 0.11$ eV, only the $1+$, $1-$, and $3-$ charge states can exist thermally. These

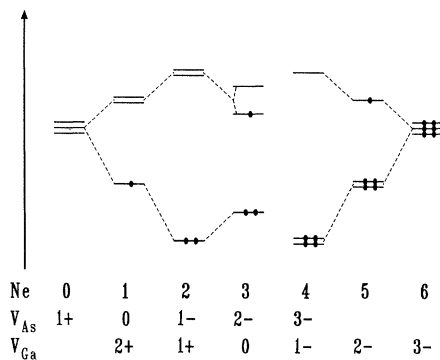


FIG. 2. Level splitting vs the electron filling N_e of a triply degenerate gap state under a Jahn-Teller distortion. The configurations correspond to the minima of the total energies as calculated in Ref. 19. The corresponding charge states in the cases of V_{As} and V_{Ga} are indicated.

states are all diamagnetic, i.e., are invisible by EPR experiments. The smallness of the calculated effective Coulomb energy (≈ 0.13 eV) explains why negative- U systems can be so easily obtained.

From positron annihilation experiments, it seems that native vacancy defects exist with a concentration of the order of $10^{17}-10^{18}$ cm^{-3} .²⁰⁻²² In Ref. 22 the positron trapping and annihilation were observed to be strongly dependent on the position of the Fermi level. The authors have found two Fermi level controlled transitions at $E_c=0.035$ eV and $E_c-0.10$ eV. They have proposed that these levels could correspond to $\epsilon(2-/1-)$ and $\epsilon(1-/0)$. Furthermore, there is a large number of experimental results on irradiation defects in GaAs.^{23,24} In n -type GaAs, five electron centers (E_1-E_5) and two hole centers (H_0, H_1) are observed by deep-level transient spectroscopy (DLTS) or deep-level optical spectroscopy (DLOS) $E_3-E_4-E_5$ are associate with $V_{As}-As_i$ pairs where As_i is an arsenic interstitial. The authors have proposed to identify E_1 and E_2 with the $\epsilon(2-/1-)$ and $\epsilon(1-/0)$ levels of the isolated vacancy V_{As} , in particular by comparison with the theoretical results of Bachelet, Baraff, and Schlüter.¹ The experimental E_1 and E_2 levels are, respectively, at $E_c-0.04$ eV and $E_c-0.18$ eV. The localization of the ionization levels of V_{As} in the upper part of the band gap is in agreement with our results. But our $\epsilon(2-/1-)$ and $\epsilon(1-/0)$ levels are slightly lower in the gap than the proposed ones. Furthermore, the difference between the two calculated levels is always larger than 0.11 eV—the Coulomb energy—and increases with the Jahn-Teller energy. Therefore the identification of the $E_c-0.035$ eV and $E_c-0.10$ eV levels²² is doubtful as regard to our results. Instead, we could propose $\epsilon(3-/2-)$ and $\epsilon(2-/1-)$ which are higher in energy. As the experimental difference between the levels is only 0.065 eV, we should suppose a small Jahn-Teller relaxation ($\Delta < 0.03$ eV, see Fig. 1). Further experiments are needed to bring new information.

Finally, we can look at what could be the EPR properties of V_{As} , assuming that a paramagnetic state is thermally stable. As already said, for the t_2 state of V_{As}^0 , 47% of the wave function is localized on the first neighbors. Among this, 51% is s -like. These localization factors do not vary too much with the occupancy of the deep state. The s localization is very important and is confirmed by other calculations.^{7,17} But his information is not sufficient. In effect, depending on the nature of the distortion, the electron will be mainly localized on one, two, three, or four neighbor atoms. Let us investigate the case of V_{As}^0 whose t_2 level is populated by one electron. The system is characterized by a tetragonal or a trigonal distortion.^{14,25} As in the case of the positive vacancy in Si, we an try to describe the system with a one-electron molecular model.²⁵ In the case of a tetragonal distortion, the paramagnetic electron occupies a molecular orbital wave function of the form $\frac{1}{2}(a-b-c+d)$ where a, b, c, d are the four dangling bonds. In the case of a trigonal distortion, it is of the form $(1/\sqrt{12})(3a-b-c-d)$. These results mean that for a tetragonal distortion the electron is localized on the four neighbors and for a trigo-

nal distortion mainly on only one neighbor (in a first-order theory). The g tensor is axially symmetric in the two cases, but, respectively, in the [100] and [111] directions for the tetragonal and trigonal distortions. To our knowledge, such spectra have never been observed. For V_{As}^{2-} (3 electrons in the t_2 state), this is more complex since mixed distortions are expected.

In all our calculations we have supposed that the Jahn-Teller effect is more important than the many-body interactions (see the case of the gallium vacancy in GaP).²⁶ In effect, EPR spectra have been reported in irradiated GaAs and associated with the arsenic vacancy.²⁴ The spectra are well fitted with an $S = 1$ spin Hamiltonian which means that exchange effects could be important. But the hyperfine interactions are not resolved. Therefore, a more detailed analysis of these experimental spectra and of the complicated problem of the many-electron interactions is needed to conclude.

IV. GALLIUM VACANCY IN GaAs

For the gallium vacancy in GaAs, we have calculated four ionization levels: $\epsilon(3-/2-) = 0.57$ eV, $\epsilon(2-/1-) = 0.39$ eV, $\epsilon(1-/0) = 0.25$ eV, and $\epsilon(0/1+) = 0.13$ eV. This is in rather good agreement with the local density results of Baraff and Schlüter² with the exception that the positive charge state is not stable in their calculation. The charge states correspond to a different filling of the t_2 state which is lower in the gap compared to the arsenic vacancy. This is in agreement with other calculations.^{1,7,16,17} The neutral gallium vacancy is characterized by three electrons on the t_2 state (see Fig. 2). The lattice distortions have been considered in the same manner as for V_{As} . The levels are plotted in Fig. 3 with respect to the Jahn-Teller energy Δ . The 0 and 2- charge states are not thermally stable for, respec-

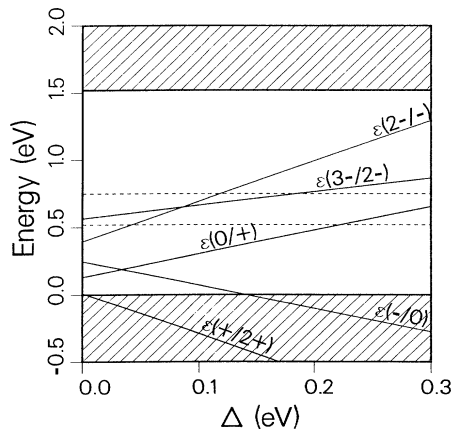


FIG. 3. Ionization levels for the distorted gallium vacancy in GaAs. The levels are represented as function of the Jahn-Teller energy Δ . The top of the valence band is taken as reference for the energies. For comparison, the experimental levels associated with EL2 are plotted by dashed lines.

TABLE I. s , p , and total localizations of the t_2 wave function on the first neighbors for the gallium vacancy in GaAs.

Charge state	s	p	Total
3-	0.10	0.51	0.61
2-	0.09	0.52	0.61
1-	0.08	0.51	0.59
0	0.07	0.49	0.56
1+	0.06	0.45	0.51

tively, $\Delta > 0.03$ eV and $\Delta > 0.09$ eV because of negative- U situations. The localizations of the t_2 wave function on the first neighbors are given in Table I for the various charge states. We see that the total localization is of order of 55% on the first neighbor atoms, mainly with a p character in agreement with Refs. 7 and 17. This is an important difference with V_{As} .

Recently, an EPR signal has been observed at the thermal equilibrium in irradiated GaAs samples and interpreted as V_{Ga}^{2-} .²⁷ The spectrum has a trigonal symmetry along the [111] direction. It is described by a spin Hamiltonian with $S = \frac{1}{2}$ and $I = \frac{3}{2}$, the hyperfine interaction being typical of only one As atom (one isotope, $A_{\parallel} = 280 \times 10^{-4}$ cm⁻¹, $A_{\perp} = 130 \times 10^{-4}$ cm⁻¹). A rough estimate of the electron localizations from the hyperfine parameters gives, respectively, 4 and 45 % of s and p densities of the paramagnetic electron on the As atom. V_{Ga}^{2-} is characterized by 5 electrons on the t_2 state. With the electron-hole symmetry,¹⁹ we know that this problem can be treated as with one electron on the t_2 state, a problem which has been discussed in the previous section for V_{As}^0 . Taking in account the symmetry of the g and hyperfine tensors, we assume a trigonal distortion of V_{Ga}^{2-} . The molecular wave function of the paramagnetic electron has the form $(1/\sqrt{12})(3a - b - c - d)$. Using the electron localizations for V_{Ga}^{2-} in Table I, we obtain, respectively, 7 and 39 % for the s and p localizations on atom a which are in good agreement with the experimental values, taking into account that the distortion can modify the s density.²⁸ Furthermore, the V_{Ga} EPR spectrum is seen in some samples with the As_{Ga}^+ —or EL2—signal.²⁷ Thus we know that the Fermi level lies between the (0/1+) and (1+/2+) levels of As_{Ga} (or the corresponding levels of EL2). These levels are found experimentally at $E_v + 0.52$ eV and $E_v + 0.75$ eV (Ref. 29) and are indicated by dashed lines in Fig. 3. We see in Fig. 3 that the stability zone of V_{Ga}^{2-} is compatible with this Fermi level location if we assume a small lattice relaxation ($\Delta < 0.09$ eV).

V. ARSENIC ANTISITE

The arsenic antisite As_{Ga} has been extensively studied, particularly because it is involved in the atomic structure of EL2.³⁰ EL2 is probably the most studied defect in GaAs but its atomic structure is still controversial. Mainly two models are proposed: the isolated antisite³

and the arsenic-antisite arsenic interstitial pair $\text{As}_{\text{Ga}}\text{-As}_i$.^{31,32} In this paper our aim is not to discuss about *EL2* which is already the subject of an important literature (for a review, see Ref. 30, for example).

The electronic structure of As_{Ga} is well known. The interaction of the *s* and *p* orbitals of the antisite with its neighbors leads to bonding and antibonding states. The antibonding a_1 state lies in the band gap and gives rise to two occupancy levels in the gap: $\epsilon(1+/2+)$ and $\epsilon(0/1+)$. The neutral state corresponds to a completely filled a_1 state (2 electrons). We calculate $\epsilon(0/1+)=1.37$ eV and $\epsilon(1+/2+)=1.20$ eV. This is in good agreement with the local-density results of Baraff and Schlüter.² But it is 0.7-eV higher than the experimental levels which are associated with *EL2*.²⁹ The electron density on the *s* orbital of the antisite is about 18% for the three charge states. This localization is very close to the experimental value 18.2%, which can be deduced from the hyperfine interaction $A=890\times 10^{-4}$ cm⁻¹ obtained by Wörner, Kaufman, and Schneider using the electron spin resonance technique.³³

VI. GALLIUM ANTISITE

In comparison with the arsenic antisite, little is known about the electronic states of the gallium antisite Ga_{As} . An acceptor with energy levels at 77 and 230 meV from the valence band edge has been attributed to $\epsilon(1-/0)$ and $\epsilon(2-/1-)$ of Ga_{As} .³⁴ Similarly, a double acceptor with energy levels at 78 and 203 meV has been observed in nonstoichiometric GaAs ($\text{Ga}_{0.55}\text{As}_{0.45}$) and has been interpreted in the same manner.³⁵ Recently³⁶ the nature of these acceptor states has been reexamined in *n*-type and *p*-type Ga-rich GaAs samples. An important difference is observed between *n*-type and *p*-type samples, the intensity ratio of the two DLTS peaks corresponding to the two levels being inverted. An explanation has been given recently by Zhang and Chadi⁴ who calculated the stable atomic configuration of Ga_{As} in its different charge states. For the undistorted system, they have found a threefold-degenerate t_2 level which can be filled by 4, 5, and 6 electrons for Ga_{As}^0 , Ga_{As}^- , and $\text{Ga}_{\text{As}}^{2-}$. This picture for the undistorted defect is identical to the results of Ref. 2. In the neutral state, the system is subject to a very strong relaxation which leads to a negative-*U* system [$\epsilon(2-/1-)<\epsilon(1-/0)$]. This negative-*U* situation could explain the experimental results of Ref. 30.

In our case we calculate the t_2 level always lying in the valence band, which means that the antisite is always in the doubly negative charge state. This is in disagreement with the previous results^{2,4} but in agreement with the tight-binding calculations of Ref. 16. Nevertheless, our t_2 level is close to the top of the valence band: it is reasonable to think that our $\epsilon(2-/1-)$ and $\epsilon(1-/0)$ levels could be pushed in the band gap if the distortions were considered. One must also point out that a hole trap with energy levels at $E_v+0.4$ eV and $E_v+0.7$ eV is reported in the literature and also assigned to Ga_{As} .^{37,38} Our results give a stronger support to the assignation of the (78/203 meV) levels to Ga_{As} . Anyway, several Ga_{As} related defects differing by their magnetic circular

dichroism of the absorption have been reported.^{37,39} The isolated antisite Ga_{As} or more complex defects $\text{Ga}_{\text{As}}\text{-X}$ are possible candidates. Therefore the association of the (78/203 meV) levels with the isolated Ga_{As} is still far from certain.

VII. GALLIUM INTERSTITIAL

To our knowledge, there is only one paper giving experimental information about the gallium interstitial Ga_i .⁴⁰ It concerns an optically detected magnetic resonance spectrum in $\text{Al}_x\text{Ga}_{1-x}\text{As}$ ($x=0.26$) which is characterized by a central hyperfine splitting $A(^{69}\text{Ga})=0.050$ cm⁻¹ and $A(^{71}\text{Ga})=0.064$ cm⁻¹. This strong hyperfine coupling is said to be typical of an electronic state of A_1 symmetry with a localization of about 12% on the central atom. The spectrum is slightly anisotropic, indicating that Ga_i is probably paired with a second defect.

We have calculated the electronic structure of the interstitial at both sites of T_d point-group symmetry and at the hexagonal site (designated as *H*). We use the same notations as in Ref. 2: T_{d1} (T_{d2}) is the site of T_d point-group symmetry for which the four nearest neighbors are As (Ga) atoms. The ionization levels for the three sites are given in Table II. For the interstitial at the T_{d2} site, we have found no deep state in the gap and the defect is always in the positive charge state. This is totally in agreement with the local density results of Baraff and Schlüter.² At the T_{d1} site we have calculated a shallow $\epsilon(1+/2+)$ level close to the valence band, at $E_v+0.02$ eV. In Ref. 2, the $\epsilon(1+/2+)$ and $\epsilon(2+/3+)$ levels are obtained in the lower part of the gap. These levels have an a_1 symmetry. In the positive charge state, the a_1 level is completely filled. Our results show that maybe there is no deep level associated with the gallium interstitial in GaAs and that the defect is always in a diamagnetic state, i.e., is EPR invisible. It could be an explanation why there is no observation of Ga_i in GaAs, in addition to the fact that the defect could be often in a very low concentration.² Our calculated a_1 state is strongly localized on the *s* orbital of the interstitial atom, about 42%. So it is very difficult to explain the low experimental value, 12%, obtained in GaAlAs.⁴⁰ The interstitial atom is maybe strongly paired with another defect. A second possibility is that the observed defect is not associated with the gallium interstitial. We could propose, for example, the arsenic vacancy for which the theory also predicts a strong *s* density on the gallium atoms. A better description of the symmetry of the experimental spin

TABLE II. Ionization levels of the gallium interstitial Ga_i at the sites T_{d1} , T_{d2} with T_d point-group symmetry and at the hexagonal site *H* (notations are explained in the text). The energies are referred to the top of the valence band.

	T_{d1}	T_{d2}	<i>H</i>
1+/2+	0.02	VB	0.37
0/1+	CB	CB	1.38

Hamiltonian is needed for a clear identification.

We have also investigated the case of the interstitial at the hexagonal site (H). The H site interstitial is expected to be unstable compared to the two tetrahedral sites T_{d1} and T_{d2} .⁴¹ Maybe it is metastable or it becomes stable when it is coupled with other defects. Therefore it is interesting to study its electronic structure. The gallium interstitial at the H site is characterized by two a_1 states in the gap (in C_{3v} point-group symmetry). For the defect in the neutral charge state, for example, we calculate the a_1 levels at $E_v + 0.79$ eV and $E_v + 1.41$ eV. They are, respectively, populated by two and one electrons. The s and p densities (n_s, n_p) on Ga_i are (0.38, 0.01) for the lowest level and (0.01, 0.33) for the highest one. The highest a_1 level is thus strongly p type: it comes from the splitting of the original t_2 state. As seen in Table II we show that three charge states are possible: $2+$, $1+$, and 0 .

VIII. ARSENIC INTERSTITIAL

As for the gallium interstitial, there is no experimental evidence concerning the electronic structure of the arsenic interstitial As_i . Recently, Christoffel *et al.*⁴² have reported an EPR spectrum which is separable in two spectra both attributed to As interstitial-related defects. Furthermore, the defects in irradiated GaAs are often interpreted as complexes between an arsenic vacancy and an arsenic interstitial.^{23,24} But to our knowledge, the isolated arsenic antisite has never been observed unambiguously. We have performed the calculation for the three sites T_{d1} , T_{d2} , and H . For the two tetrahedral sites (T_{d1} and T_{d2}) we get very similar results. The electronic structure is characterized by a deep t_2 state which is not populated for the defect in the triply positive charge state. We calculated the $\epsilon(2+/3+)$ and $\epsilon(1+/2+)$ levels at, respectively, $E_v + 1.05$ (0.99) eV and $E_v + 1.28$ (1.27) eV for the interstitial at the T_{d1} (T_{d2}) site. Our results are very close to those of Ref. 2 in the case of the site T_{d1} but the agreement is poorer in the case of T_{d2} [they obtain an $\epsilon(0/1+)$ level near 1.3 eV]. As the t_2 state is triply degenerate, the system must be subject to Jahn-Teller distortions in the $+$ and $2+$ charge states. As we have done for V_{As} and V_{Ga} , using the theory of Ref. 19, we have calculated the influence of the distortions on the defect level positions.

One must note that contrary to the case of the vacancy, the energy may not be a symmetric function of the displacement, if the interstitial moves along $\langle 111 \rangle$ directions, for example. Such a nonsymmetric situation is also examined in Ref. 19. Fortunately, the equations of the occupancy levels are the same in the symmetric and nonsymmetric cases for the occupancy numbers considered here (see Ref. 19 for details). The levels are plotted in Figs. 4 and 5. We see that for $\Delta \gtrsim 0.13$ eV a negative- U situation occurs ($\epsilon(2+/3+) > \epsilon(1+/2+)$). In that case, the paramagnetic $2+$ charge state is not thermally stable and the defect is EPR invisible. Thus, as pointed out in Ref. 19, the nonobservation of the arsenic interstitial could be explained by Jahn-Teller distortions. The arsenic interstitial at the hexagonal site is characterized

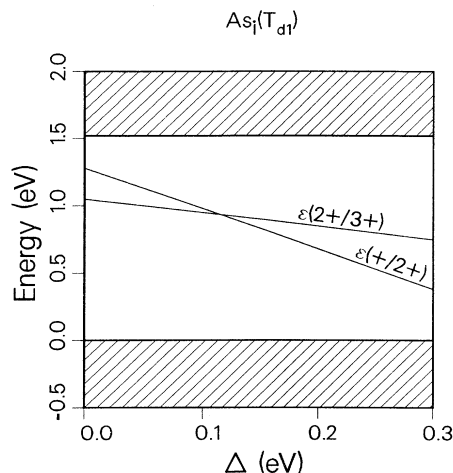


FIG. 4. Ionization levels for the distorted arsenic interstitial at the T_{d1} site in GaAs (see text for notations). The levels are represented as function of the Jahn-Teller energy Δ . The top of the valence band is taken as reference for the energies.

by an a_1 level in the band gap. This state results from the splitting of the t_2 state into a_1 and e states. The e state is higher in energy and lies in the conduction band. For the positive charge state, the a_1 level is populated by two electrons. We calculate an $\epsilon(1+/2+)$ level at $E_v + 0.13$ eV. The net s and p densities on the interstitial atom are, respectively, 1.8 and 52.8 %.

Now we can consider the EPR properties of the arsenic interstitial. For the defect at the T_{d1} and T_{d2} sites, the t_2 state has a localization factor about 36% on the p orbitals of the As_i atom. The effect of the distortions will be probably to mix some s density (a few percent) but we do not expect that the total density will change dramatically.

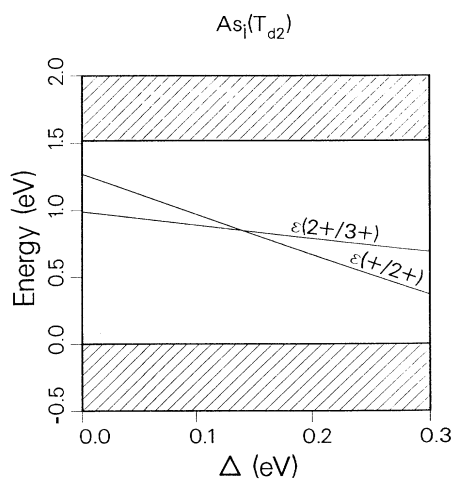


FIG. 5. Same as Fig. 4 for the arsenic interstitial at the T_{d2} site.

With these results in mind, let us have a look at the two defects reported by Christoffel *et al.*⁴² (they are labeled *ST1* and *ST2*). The observed trigonal symmetry could be possible for an interstitial defect distorted along the (111) directions. But the *s* and *p* densities that we can estimate from the hyperfine interactions are, respectively $(4.30 \pm 0.15)\%$ and $(9.00 \pm 6.00)\%$ for the defect *ST1*, $(1.77 \pm 0.12)\%$ and $(6.00 \pm 4.50)\%$ for *ST2*. Thus the total density is always at least two times lower than the calculated one. We can conclude that the observed defect is more probably a complex involving an arsenic interstitial.

IX. GALLIUM ANTISITE GALLIUM VACANCY PAIR

The problem of the atomic configuration of the vacancies in GaAs has been examined in the last sections using the predictions of the Jahn-Teller theorem. But it is not obvious that such a simple theory can effectively predict the stable atomic configuration of a defect. In particular, a vacancy can be strongly unstable relative to the displacement of one of the neighbor atoms. This leads in an extreme situation to an antisite vacancy pair when the neighbor atom fills the vacancy site. In this section we present results about $\text{Ga}_{\text{As}}-\text{V}_{\text{Ga}}$ which could be the stable or metastable state of the arsenic vacancy V_{As} . In Ref. 43, Baraff and Schlüter have found using total energy calculations that the pair $\text{Ga}_{\text{As}}-\text{V}_{\text{Ga}}$ is stable relative to V_{As} at high Fermi energy (> 0.9 eV). Thus we can look at the electron densities associated with this pair defect.

The calculated electronic structure of $\text{Ga}_{\text{As}}-\text{V}_{\text{Ga}}$ is characterized by a deep twofold degenerate *e* level which is strongly derived from the t_2 state of V_{Ga} . The *e* states are localized on the three As atoms around the gallium vacancy. We calculate a localization about 52% on these three As atoms and only 0.1% on the antisite Ga atom. Therefore, the pair defect has the same electronic structure as the gallium vacancy with the exception that the electron density is shared on only three neighbors. In the neutral state the *e* level is populated by one electron. The predicted charge states are $3-$, $2-$, $1-$, and 0 . We obtain $\epsilon(3-/2-)=0.55$ eV, $\epsilon(2-/1-)=0.35$ eV, and $\epsilon(1-/0)=0.16$ eV. These levels are ≈ 0.4 eV lower than those calculated by Baraff and Schlüter⁴³ but the electronic structure is quite similar. The defect symmetry of the defect in our calculation is C_{3v} . This symmetry can be lowered due to Jahn-Teller distortions which are expected due to the twofold degenerescence of the *e* level. Therefore the resulting electron density is not necessarily equally shared on the three As atoms but can be on only one or two atoms (see the discussion about the As and Ga vacancies).

X. ARSENIC ANTISITE ARSENIC VACANCY PAIR

The bistability and metastability of the gallium vacancy to form $\text{As}_{\text{Ga}}-\text{V}_{\text{As}}$ has been proposed as a possible model for *EL2*.^{44,45} The striking point is to know if the paramagnetic state is As_{Ga} -like or V_{As} -like. We have calculated the electronic structure of $\text{As}_{\text{Ga}}-\text{V}_{\text{As}}$ in the $3+$, $2+$, $+$, 0 , $-$ charge states. The one-electron level structure for the neutral defect is shown on Fig. 6. There are

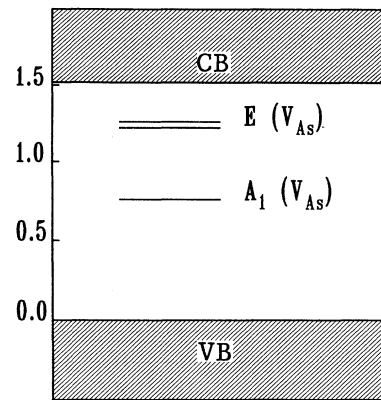


FIG. 6. Electronic structure of the $\text{As}_{\text{Ga}}-\text{V}_{\text{As}}$ pair defect. In the neutral state, the lowest a_1 level is populated by two electrons, the *e* level by one electron.

two deep levels in the band gap which are strongly V_{As} -like, i.e., they are localized on the three Ga neighbor atoms of the vacancy. There is an a_1 level in resonance in the conduction band which has mainly an As_{Ga} character. In the neutral charge state, the lowest a_1 level is populated by two electrons, the *e* level by one electron. Thus our conclusions are close to those of Ref. 45. The paramagnetic state is always V_{As} -like. Our calculated levels are $\epsilon(2+/3+)=0.22$ eV, $\epsilon(1+/2+)=0.36$ eV, $\epsilon(0/1+)=1.00$ eV, and $\epsilon(1-/0)=1.16$ eV. The $\epsilon(1-/0)$ and $\epsilon(0/1+)$ levels are less certain because the defect must distort in the neutral and singly negative charge states.

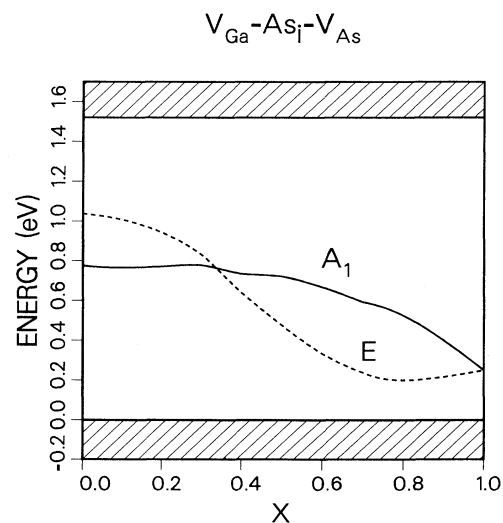


FIG. 7. Evolution of the one-electron levels of the $\text{V}_{\text{Ga}}-\text{As}_i-\text{V}_{\text{As}}$ defect in the neutral charge state with respect to the position *x* of the interstitial atom As_i (notations are explained in the text).

Von Bardeleben, Bourgoïn, and Miret have reported the observation of an irradiation-induced defect in *n*-type GaAs.⁴⁶ The spectrum is attributed to $\text{As}_{\text{Ga}}-\text{V}_{\text{As}}$ because the large central hyperfine constant (0.068 cm^{-1}) is typical of an arsenic antisite. But our calculations and those of Ref. 45 have shown that the paramagnetic state of $\text{As}_{\text{Ga}}-\text{V}_{\text{As}}$ is strongly V_{As} -like (nevertheless, as shown below, the *s* density is equally shared between As_i and V_{As}). It has been proposed that the As ion could not be necessarily at the Ga site but at an intermediate position between the Ga and As sites.⁴⁶ Consequently, we have calculated the electronic levels of the defect $\text{V}_{\text{Ga}}-\text{As}_i-\text{V}_{\text{As}}$ with respect to the position *x* of the arsenic atom As_i . We take $x=0$ when As_i is at the Ga site ($\text{As}_{\text{Ga}}-\text{V}_{\text{As}}$) and $x=1$ when As_i is at the As site (V_{Ga}). We analyze here the results for the neutral defect but the conclusions about the electron densities are similar for the various charge states. As shown in Fig. 7 there are two levels with a_1 and e symmetry in the band gap. For $x=1$, the two levels are degenerate and correspond to the t_2 level of V_{Ga} . A crossing of the two levels occurs for $x \approx 0.35$. In Table III we give the a_1 and e level energies for x between 0 and 0.7. We also report the total and *s* localizations of the a_1 on the As_i atom, on the three As neighbor atoms of V_{Ga} , and on the three Ga neighbor atoms of V_{As} . We see in Table III that the a_1 wave function is V_{As} -like when $x=0$ and V_{Ga} -like when $x > 0.5$. The *s* densities vary importantly with x . The expected EPR spectrum for such a defect would be typical of the atom which has the higher *s* density for the paramagnetic state. For that purpose we can compare the *s* densities per atom (for V_{Ga} and V_{As} the density is equally shared on three atoms). For $x=0$, the *s* density is equal on the As_i atom and on the three Ga neighbor atoms of V_{As} ($\approx 5\%$). But when x is higher, the *s* density on As_i increases and the *s* density on V_{As} decreases. Therefore, for $x \geq 0.3$, the spectrum should be typical of one As atom, and thus could explain the experimental observation. But the *s* density on As_i is always lower than 7% and do not compare with the experimentally deduced value (14%). Furthermore, the observed defect has an ionization energy $E \leq 0.35 \text{ eV}$ from the conduction band. This is not easily made compatible with the a_1 level which always lies in the central or lowest part of the gap.

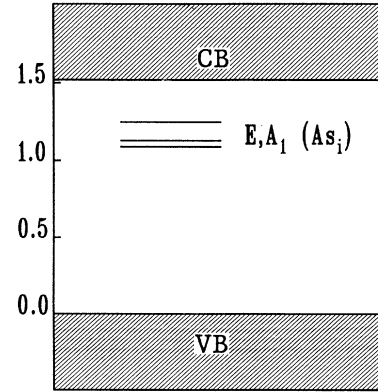


FIG. 8. Electronic structure of the $\text{Ga}_{\text{As}}-\text{As}_i$ pair defect in the positive charge state. The e and a_1 levels in the band gap are not populated.

XI. GALLIUM ANTISITE ARSENIC INTERSTITIAL PAIR

Among the various defects expected in GaAs, the antisite interstitial pairs are often proposed. One important result predicted by the theory is that the gallium and arsenic isolated interstitial defects are always in positive charge states. Therefore the interstitial atoms will probably form pair defects with the Ga antisite which is always in a doubly negative charge state in our calculation. The pairing of an interstitial atom with As_{Ga} seems to be more difficult because of the positive or neutral charge state of the antisite. We have calculated the electronic structure of the four antisite interstitial pairs: $\text{As}_{\text{Ga}}-\text{As}_i$, $\text{As}_{\text{Ga}}-\text{Ga}_i$, $\text{Ga}_{\text{As}}-\text{As}_i$, and $\text{Ga}_{\text{As}}-\text{Ga}_i$. For simplicity and because we do not treat the long-range Coulomb interactions, we have only investigated the closest pairs where the interstitial atom stands at one bond length (2.43 \AA) of the antisite in a $\langle 111 \rangle$ direction.

Let us consider now the $\text{Ga}_{\text{As}}-\text{As}_i$ case. The single-particle energies are represented in Fig. 8. There are two levels in the band gap (a_1 and e) which are derived from the original t_2 level of the As interstitial atom. The cal-

TABLE III. One-electron energies of the a_1 and e levels of the $\text{V}_{\text{Ga}}-\text{As}_i-\text{V}_{\text{As}}$ defect. The results are given versus the As_i position x ($x=0$ for $\text{As}_{\text{Ga}}-\text{V}_{\text{As}}$ and $x=1$ for V_{Ga}). The total and *s*-like densities of the a_1 state on the As_i atom, on the three As neighbor atoms of V_{Ga} and on the three Ga neighbor atoms of V_{As} are also reported.

x	a_1 (eV)	e (eV)	As_i total	As_i <i>s</i>	V_{Ga} total	V_{Ga} <i>s</i>	V_{As} total	V_{As} <i>s</i>
0.0	0.76	1.02	0.078	0.056	0.140	0.048	0.405	0.151
0.1	0.77	1.00	0.065	0.056	0.138	0.048	0.418	0.156
0.2	0.77	0.94	0.063	0.061	0.161	0.055	0.400	0.150
0.3	0.78	0.83	0.067	0.068	0.204	0.066	0.361	0.134
0.4	0.74	0.64	0.077	0.075	0.265	0.080	0.305	0.110
0.5	0.72	0.48	0.092	0.077	0.328	0.093	0.242	0.086
0.6	0.67	0.34	0.112	0.074	0.382	0.100	0.184	0.062
0.7	0.59	0.24	0.136	0.068	0.411	0.100	0.141	0.045

culated charge states are $1+$, 0 , $1-$ corresponding to 0 , 1 , and 2 electrons on the e level. The p localizations of the e and a_1 states on the arsenic interstitial are, respectively, 25 and 29% (for the a_1 state the s localization is lower than 1%). On the gallium antisite, the localization is always lower than 3% . In conclusion, our calculation shows that the $\text{Ga}_{\text{As}}\text{-As}_i$ pair has an electronic structure close to the arsenic interstitial one. The p density is rather important ($\approx 25\%$). $\text{Ga}_{\text{As}}\text{-As}_i$ cannot be the defect observed by Christoffel *et al.*⁴² because the experimental total density is lower than 14% (see Sec. VIII). One must also point out that recent total energy calculations⁴ give a large binding energy for the pair but a small 0.3-eV barrier for the $\text{Ga}_{\text{As}}\text{-As}_i$ interchange reaction.

XII. GALLIUM ANTISITE GALLIUM INTERSTITIAL PAIR

Our calculation predicts an a_1 level in the lowest part of the band gap for the $\text{Ga}_{\text{As}}\text{-Ga}_i$ pair defect. This level corresponds to the a_1 level of the gallium interstitial. It is strongly localized on the interstitial (37%) and slightly on the antisite (5%). The electron density is mainly s -like so that the hyperfine tensor of such a defect should be characterized by a huge contact term (around 0.15 cm^{-1}). We calculate $\epsilon(1-/0)=0.34\text{ eV}$ and $\epsilon(0/1+)=0.02\text{ eV}$. The a_1 level is empty in the positive charge state. To our knowledge, such a defect has never been observed.

XIII. ARSENIC ANTISITE GALLIUM INTERSTITIAL PAIR

The one-particle levels of the $\text{As}_{\text{Ga}}\text{-Ga}_i$ pair defect are pictured in Fig. 9. There is only one level in the gap whose symmetry is a_1 . This state has mainly the character of the arsenic antisite (between 16 and 18% on the s orbital of As_{Ga}). It is not populated when the defect is in the $3+$ charge state. The calculated ionization levels are $\epsilon(2+/3+)=0.96\text{ eV}$ and $\epsilon(1+/2+)=1.25\text{ eV}$. The doubly positive charge state is paramagnetic and should be characterized by a similar EPR spectrum as the isolated arsenic antisite. There are several defects reported in the literature which have an As_{Ga} -like EPR spectrum. First, as discussed in Sec. X, such a defect has been observed by EPR and first attributed to the $\text{As}_{\text{Ga}}\text{-V}_{\text{As}}$ pair.⁴⁶ The dominant donor in GaAs, *EL2*, has also the same signature.³⁰ Recently, it has been shown by plastic deformation of GaAs that arsenic antisite defects are created and show a similar optically detected electron spin-resonance pattern as *EL2* defects.⁴⁷ But the new antisite defects can be distinguished by their different spectral dependence of the magnetic circular dichroism (MCD). From our study we see that the $\text{As}_{\text{Ga}}\text{-Ga}_i$ pair defect could be one of the observed effects. In particular, as seen in Fig. 9, the pair defect is characterized by a_1 and e levels in the conduction band and by an a_1 level in the valence band. These resonant states could explain the differences in the MCD. But we should prove the stability of the $\text{As}_{\text{Ga}}\text{-Ga}_i$ pair.

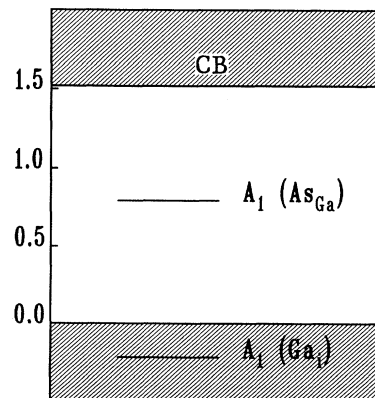


FIG. 9. Electronic structure of the $\text{As}_{\text{Ga}}\text{-Ga}_i$ pair defect in the triply positive charge state. The a_1 level in the band gap is not populated.

XIV. ARSENIC-ANTISITE ARSENIC INTERSTITIAL PAIR

The $\text{As}_{\text{Ga}}\text{-As}_i$ pair has been extensively studied because it represents one of the main models for *EL2*.^{30,41,48} Here we have only investigated the pair in which the interstitial atom is at one bond length from the antisite (called T^* in Ref. 41). The electronic structure calculated for the defect is pictured in Fig. 10. There are three states in the band gap: one bonding a_1 state and one antibonding a_1 state which result from the interaction of the a_1 state of As_{Ga} with the t_2 state of As_i , and one e state which is totally derived from the t_2 state of As_i . This picture is totally in agreement with the calculations of Ref. 41. But our stable charge states are $5+$, $4+$, $3+$, and $2+$ which is in total discrepancy with the same refer-

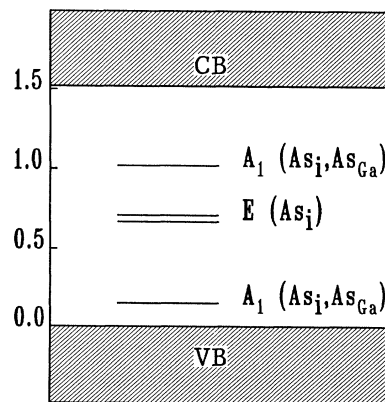


FIG. 10. Electronic structure of the $\text{As}_{\text{Ga}}\text{-As}_i$ pair defect in the $5+$ charge state. The levels in the gap are not populated.

ence (they obtain the $2+$, $1+$, and 0 charge states). One possible explanation for this difference is that our calculation is not really suited for the defects with very ionized charge states since the interatomic Coulomb interactions are not considered. The bonding and antibonding a_1 states and the e state are empty in the $5+$ charge state. We obtain $\epsilon(4+/5+)=0.31$ eV, $\epsilon(3+/4+)=0.66$ eV, and $\epsilon(2+/3+)=1.22$ eV. The $4+$ and $2+$ charge states are paramagnetic. In the $4+$ charge state, the unpaired electron is on the a_1 bonding state whose s and p densities are, respectively, 0.5% (12.8%) and 23.1% (0.2%) on the As_i (As_{Ga}) atom. Therefore the EPR spectrum should be typical of As_{Ga} . In the $2+$ state, the unpaired electron is on the e state. A distortion of the sys-

tem must be predicted. We refer to Ref. 48 for more details about distortions of this defect.

XV. CONCLUSION

The electronic structure of several isolated and complex intrinsic defects in GaAs is calculated. The electron densities are given to help for a possible identification of these defects by EPR techniques. The discussion of already observed EPR spectra is made in view of these results. The overall agreement with results obtained by local-density techniques is good. This leads us to conclude that the self-consistent tight-binding technique is promising for further studies of more complex defects.

-
- ¹G. B. Bachelet, G. A. Baraff, and M. Schlüter, Phys. Rev. B **24**, 915 (1981).
²G. A. Baraff and M. Schlüter, Phys. Rev. Lett. **55**, 1327 (1985).
³J. Dabrowski and M. Scheffler, Phys. Rev. Lett. **60**, 2183 (1988); D. J. Chadi and K. J. Chang, *ibid.* **60**, 2187 (1988).
⁴S. B. Zhang and D. J. Chadi, Phys. Rev. Lett. **64**, 1789 (1990).
⁵M. Lannoo, J. Phys. C **17**, 3137 (1984).
⁶C. Delerue, M. Lannoo, and G. Allan, Phys. Rev. B **39**, 1669 (1989).
⁷Hongqi Xu and U. Lindefelt, Phys. Rev. B **41**, 5979 (1990).
⁸J. Petit, M. Lannoo, and G. Allan, Solid State Commun. **11**, 861 (1986).
⁹T. Bretagnon, G. Bastide, M. Rouzeyre, C. Delerue, and M. Lannoo, Phys. Rev. B **42**, 11 042 (1990).
¹⁰D. N. Talwar and C. S. Ting, Phys. Rev. B **25**, 2660 (1982).
¹¹M. Lannoo and P. Lenglar, J. Phys. Chem. Solids **30**, 2409 (1969).
¹²W. A. Harrison, Phys. Rev. B **24**, 5835 (1981).
¹³I. Lefebvre, M. Lannoo, G. Allan, and L. Martinage, Phys. Rev. B **38**, 8593 (1988).
¹⁴M. Lannoo and J. Bourgoin, in *Point Defects in Semiconductors I*, edited by M. Cardona (Springer, Berlin, 1981).
¹⁵J. C. Slater, *Quantum Theory of Atomic Structure* (McGraw-Hill, New York, 1960).
¹⁶P. J. Lin-Chung and T. L. Reinecke, Phys. Rev. B **27**, 1101 (1983).
¹⁷J. van der Rest and P. Pêcheur, J. Phys. C **17**, 85 (1984).
¹⁸G. A. Baraff, E. O. Kane, and M. Schlüter, Phys. Rev. Lett. **43**, 956 (1979); Phys. Rev. B **21**, 3563 (1980).
¹⁹M. Lannoo, Phys. Rev. B **36**, 9355 (1987).
²⁰J. L. Cheung, J. P. Karins, J. V. Corbett, and L. C. Kimerling, J. Appl. Phys. **50**, 2962 (1979).
²¹S. Dannefaer and D. P. Kerr, J. Appl. Phys. **60**, 591 (1986).
²²C. Corbel, M. Stucky, P. Hautojärvi, K. Saarinen, and P. Moser, Phys. Rev. B **38**, 8192 (1988).
²³D. Stievenard, X. Boddart, J. C. Bourgoin, and H. J. von Bardeleben, Phys. Rev. B **41**, 5271 (1990); S. Loualiche, A. Nouailhat, G. Guillot, and M. Lannoo, *ibid.* **30**, 5822 (1984).
²⁴H. J. von Bardeleben and J. C. Bourgoin, Phys. Rev. B **33**, 2890 (1986).
²⁵G. D. Watkins, in *Radiation Damage and Defects in Semiconductors 1972*, edited by J. E. Whitehouse (Institute of Physics, London, 1973), p. 228.
²⁶T. A. Kennedy, N. D. Wilsey, J. J. Krebs, and G. H. Stauss, Phys. Rev. Lett. **50**, 1281 (1983).
²⁷Y. Q. Jia, H. J. von Bardeleben, D. Stievenard, and C. Delerue (unpublished).
²⁸M. Lannoo and P. Friedel, *Atomic and Electronic Structure of Surfaces. Theoretical Foundations* (Springer-Verlag, Berlin, in press).
²⁹E. R. Weber, H. Ennen, U. Kaufmann, J. Windscheif, J. Schneider, and T. Wasinski, J. Appl. Phys. **53**, 6140 (1982).
³⁰S. Makram-Ebeid, P. Langlade, and G. M. Martin, in *Proceeding of the Third Conference on Semi-Insulating III-V Materials, 1985*, edited by D. C. Look and J. S. Blakemore (Shiva, Nantwich, England, 1985), p. 184.
³¹H. J. von Bardeleben, D. Stievenard, J. C. Bourgoin, and A. Huber, Appl. Phys. Lett. **47**, 970 (1985).
³²C. Delerue, M. Lannoo, D. Stievenard, H. J. von Bardeleben, and J. C. Bourgoin, Phys. Rev. Lett. **59**, 2875 (1987).
³³R. Wörner, U. Kaufman, and J. Schneider, Appl. Phys. Lett. **40**, 141 (1982).
³⁴Phil Won Yu, W. C. Mitchel, M. G. Mier, S. S. Li, and W. L. Wang, Appl. Phys. Lett. **41**, 532 (1982).
³⁵G. Roos, A. Schöner, G. Pensl, K. Krambrock, B. K. Meyer, J. -M. Spaeth, and J. Wagner, *Materials Science Forum*, (Trans Tech Publications, Switzerland, 1989), Vol. 38-41, p. 951.
³⁶M. Bugajski, K. H. Ko, J. Lagowski, and H. C. Gatos, in *Proceedings of the Nineteenth International Conference on the Physics of Semiconductors, Warsaw, 1988*, edited by W. Zawadzki (Institute of Physics, Polish Academy of Sciences, 1988), p. 1063.
³⁷K. Krambrock, B. K. Meyer, and J. -M. Spaeth, Phys. Rev. B **39**, 1973 (1989).
³⁸Z. G. Wang, L. A. Ledebro, and H. G. Grimmeiss, J. Phys. C **17**, 259 (1984).
³⁹J. -M. Spaeth, K. Krambrock, and D. M. Hofmann, in *Proceedings of the 20th International Conference on the Physics of Semiconductors, Thessaloniki, Greece 1990*, edited by E. M. Anastassakis and J. D. Joannopoulos (World Scientific, Singapore, 1990).
⁴⁰T. A. Kennedy and M. G. Spencer, Phys. Rev. Lett. **57**, 2690 (1986).
⁴¹G. A. Baraff and M. Schlüter, Phys. Rev. B **35**, 6154 (1987).
⁴²E. Christoffel, T. Benchiguer, A. Goltzené, C. Schwab, Wang Guangyu, and Wu Ju, Phys. Rev. B **42**, 3461 (1990).
⁴³G. A. Baraff and M. Schlüter, Phys. Rev. B **33**, 7346 (1986).
⁴⁴J. Lagowski, M. Kaminska, J. M. Parsey, Jr., H. C. Gatos, and W. Walukiewicz, in *Gallium Arsenide and Related Com-*

- pounds 1982*, edited by G. Stillman, IOP Conference Series No. 65 (Institute of Physics, Bristol, England, 1982).
- ⁴⁵G. A. Baraff and M. Schlüter, *Phys. Rev. Lett.* **55**, 2340 (1985).
- ⁴⁶H. J. von Bardeleben, J. C. Bourgoin, and A. Miret, *Phys. Rev. B* **34**, 1360 (1986).
- ⁴⁷D. M. Hofmann, B. K. Meyer, J. -M. Spaeth, M. Wattenbach, J. Krüger, C. Kisielowski-Kemmerich, and H. Alexander, *J. Appl. Phys.* **68**, 3381 (1990).
- ⁴⁸G. A. Baraff, M. Lannoo, and M. Schlüter, *Phys. Rev. B* **38**, 6003 (1988).